Chemical Engineering Science 199 (2019) 349–358

Contents lists available at ScienceDirect

Chemical Engineering Science

journal homepage: www.elsevier.com/locate/ces

# Effects of phase transformation on properties of alumina ceramic membrane: A new assessment based on quantitative X-ray diffraction (QXRD)

Xingwen Lu [a,b,e], Jiani Yang [a], Xiaoyan Li [b], Feiyun Sun [c], Fei Wang [d,b,*], Yuanqing Chao [e,f]

[a] School of Environmental Science and Engineering, and Institute of Environmental Health and Pollution Control, Guangdong University of Technology, Guangzhou 510006, China
[b] Department of Civil Engineering, The University of Hong Kong, Pokfulam Road, Hong Kong Special Administrative Region
[c] Harbin Institute of Technology, Shenzhen Graduate School, Shenzhen Key Laboratory of Water Resource Utilization and Environmental Pollution Control, Shenzhen 518055, China
[d] School of Environment, Guangzhou Key Laboratory of Environmental Exposure and Health, and Guangdong Key Laboratory of Environmental Pollution and Health, Jinan University, Guangzhou 510632, China
[e] Guangdong Provincial Key Laboratory of Environmental Pollution Control and Remediation Technology, Sun Yat-sen University, Guangzhou 510275, China
[f] School of Environmental Science and Engineering, Sun Yat-sen University, Guangzhou 510275, China

## HIGHLIGHTS

- Lower temperature alumina based ceramic membrane was synthesized with good properties.
- The influence of alumina transformation on the physical properties of ceramic membrane was investigated.
- The crystal structure of alumna phase is critical for the membrane properties.

## ARTICLE INFO

*Article history:*
Received 26 September 2018
Received in revised form 24 December 2018
Accepted 27 December 2018
Available online 23 January 2019

*Keywords:*
Ceramic membrane
Alumina
Physical properties
Membrane flux

## ABSTRACT

Alumina ceramic membranes were synthesized by pressing boehmite into disc form and sintering at different temperatures. Quantitative X-ray diffraction (QXRD) analysis was firstly used for determining the compositions of different types of alumina in membrane products. The result quantitative determined that alumina membranes experienced a series of phase transition from boehmite → γ-alumina → δ-alumina → θ-alumina → α-alumina from 450 to 1300 °C. Below 850 °C, no significant alumina transformation (i.e. γ-alumina was the dominate phase) was detected in fabricated membranes, which corresponded to stable membrane properties (i.e. porosity, BET surface area, pore size and chemical stability). At 950–1300 °C, substantial phase transformation was detected as follows, θ-alumina significantly increased from 1.21 to 61.6% (950–1125 °C), and α-alumina increased gradually from 3.98 to 100% (1100–1300 °C). Accordingly, the substantial phase transformation lead to the significant change in membrane properties at 950–1300 °C. Lower temperature (1150 °C) membrane containing 8.2% θ-alumina and 91.8% α-alumina showed comparable properties with 1300 °C consist of 100% α-alumina sintered products due to the similar alumina composition in the products. The overall results indicated that the properties of membrane were accordingly determined by the structure and content of alumina phases in membrane products. This strategy proposed a valuable method for production of lower temperature alumina-based ceramic membrane.



## 1. Introduction

Membrane technology has developed rapidly due to their unique advantages of small footprint and high removal rates (Cowan et al., 2016). Polymeric membranes are dominating the membrane market due to their low cost. However, organic nature makes polymeric membranes not able to endure harsh conditions (e.g. high temperature and severe chemical environment) (Hubadillah et al., 2018; Kujawa et al., 2014). Thus, ceramic membrane has attracted many attentions as it has superior characteristics for long life-term, thermally stable and excellent tolerance to pH (Hubadillah et al., 2018; Gestel et al., 2003; Raman et al.,

* Corresponding author.
*E-mail address:* feiwang1984@gmail.com (F. Wang).

https://doi.org/10.1016/j.ces.2018.12.054
0009-2509/

2011; Lee et al., 2016; Weber et al., 2013), which have been widely applied in water treatment and desalination processes (Zawrah et al., 2017; Xia and Liu, 2001; Padaki et al., 2015). Materials for the manufacture of ceramic membranes commonly include metal oxides (e.g. alumina ($Al_2O_3$), titania ($TiO_2$), zirconia ($ZrO_2$), silica ($SiO_2$)), clay minerals (e.g., kaolin, mullite, dolomite, etc.) as well as natural pozzolan or a combination of these materials (Hubadillah et al., 2018; Issaoui and Limousy, 2018; Achiou et al., 2017). Among these materials, clay minerals and pozzolan are low-cost materials for the production of ceramic membranes (Mouiya et al., 2018; Achiou et al., 2018). However, most commercialized ceramic membranes are manufactured from alumina due to its various shapes for the production of hollow fiber structure, nanowire and nanoporous structure (Abdullah et al., 2018; Téllez-Vázquez et al., 2016; Vega et al., 2017). Thus, alumina membrane is one of the most widely used ceramic membranes and received more and more attention (Wei et al., 2016; Barma and Mandal, 2014; Hashimoto et al., 2018).

However, alumina form several different crystal structures, such as γ-, η-, δ-, θ-, κ-, χ- and stable α-alumina (Wang et al., 2009; Yang et al., 2010; Chang et al., 2017; Nel and de Klerk, 2009). Among them, stable α-alumina were commonly used as a raw material to produce ceramic membranes because of its excellent physical and chemical performances such as high hardness, high resistance to acid or base and high melting point (Hao et al., 2018; Lima et al., 2012; Fu et al., 2015). Due to the inadequate sintering, some of commercial alumina ceramic membranes on the market consist of various transition aluminas (such as δ-, θ- and κ-alumina). Although these transition aluminas finally transformed into α-alumina (Boumaza et al., 2009; Levin and Brandon, 1998; Lee et al., 2009), it should be noted that for alumina ceramic membrane, a calcination temperature above 1400 °C is necessary for the complete transformation to α-alumina phase (Chen et al., 2017). The high temperature is proposed to make α-alumina membrane to be a compromise between mechanical strength and porosity (Kim and Van der Bruggen, 2010; Lee and Park, 2014). Effect of sintering on the properties of the alumina membrane along with crystallization has not been studied thoroughly in the literature. Thus, a quantitative understanding of alumina transformation under thermal conditions is crucial for improving properties of ceramic membrane. In addition, the influence of alumina phase transformation on properties of ceramic membrane need to be distinguished to find out low temperature alumina membrane with fairly properties for reducing energy consumption and membrane costs.

The commonly used methods for ceramic membrane fabrication are slipping casting (Jedidi et al., 2009), tape casting (Nishihora et al., 2018; Issaoui and Limousy, 2018), pressing (Del Colle et al., 2011), extrusion (Boudaira et al., 2016; Issaoui and Limousy, 2018), chemical vapor deposition (Hemmer et al., 2012) and pyrolysis (Dong et al., 2017) combined by sintering (Hubadillah et al., 2018). Comparing to other methods, pressing method is one of the most cost-effective methods and received more attention for the fabrication of ceramic membrane. In this method, a pressing force is applied on the membrane surface to produce flat sheet membrane (Antsiferoz and Gilev, 2001) and no slurry preparation is needed (Huang et al., 1999), whereas, extrusion method is using plasticizing agent and binding agent for the production of a ceramic pulp and then make shape by extrusion (Isobe et al., 2006). Both pressing and extrusion method should then treated the shaped membrane under high-temperature conditions (Jedidi et al., 2009). Generally, ceramic membranes produced by the pressing method have well-defined characteristics, such as higher mechanical strength, uniform porosity and homogeneous physical properties over the total membrane part (Hubadillah et al., 2018).

In this study, a series of alumina-based flat sheet membrane was prepared by pressing method with further thermal treatment. Firstly, QXRD technique was used to identify their crystal structures and compositions. Then, morphologies of membrane obtained at different temperatures were observed by SEM. Porosity, pore size, BET surface areas, chemical stability, and membrane flux of alumina-based membranes obtained at different temperatures were characterized. Finally, the variation of properties of alumina ceramic membranes with the formation of different types of alumina under thermal conditions were determined.

## 2. Materials and methods

### 2.1. Materials and sample preparations

The original boehmite used to prepare ceramic membrane was purchased from Sasol Ltd. (Hamburg, Germany) with an average particle size ~45 μm. The pure phase of boehmite (AlOOH) powder was confirmed by XRD. The boehmite powder with the weight of ~1 g was pressed into pellets with 20 mm diameter and 1 mm thickness at a pressure of 70 MPa to ensure consistent compaction of powder sample and in readiness for the sintering process. The pellets were sintered at 450–1300 °C with temperature increasing rate of 5 °C/min. The retention time of thermal treatment in the furnace was controlled at 30 min under air condition. After thermal treatment, the samples were allowed to cool down to room temperature using a cooling rate of 5 °C/min for producing ceramic membrane. After sintering, the samples were air-quenched and weighted for further characterization. Five duplicate pellets at each temperature were prepared for different tests.

### 2.2. XRD analysis

The sintered pellets were grounded to less than 10 μm in the mortar before XRD analysis. The XRD data of each powder sample were recorded on a D8 Advance Diffractometer (Bruker AXS) equipped with a Cu Kα X-ray tube and a LynxEye detector. The system was calibrated by Standard Reference Material 660a (lanthanum hexaboride, $LaB_6$) (Hossain et al., 2005; Tantau et al., 2014), obtained from the United States National Institute of Standard and Technology. The diffractometer was operated at 40 kV and 40 mA, and the 2θ scan range was 10–80° with a step size of 0.02° and a scan speed of 0.5 s per step for data collection. Qualitative phase identification was performed with Eva XRD Pattern Processing software (Bruker) by matching powder XRD patterns with those retrieved from the standard Powder Diffraction Database (PDF) published by the International Centre for Diffraction Data (ICDD). The Rietveld refinements for quantitative analysis of the phase compositions were processed using the TOPAS (version 4.0) crystallographic program. To estimate the purity of 1300 °C obtained alumina membrane, a refinement method using $CaF_2$ as the internal standard (De La Torre et al., 2001; Magallanes-Perdomo et al., 2009; Rendtorff et al., 2010) was used to quantify the content of alpha alumina in the 1300 °C sintered sample.

### 2.3. SEM analysis, BET surface area and pore size determination

The as-made samples were coated with a gold/platinum mixture under vacuum for 3 min at 20 mA. The morphologies of each sample were observed by a scanning electron microscopy (SEM) equipped with a secondary electron detector (Hitachi S-3400). The pore size and surface area of samples at different temperature was measured by Coulter SA 3100 (Beckman, Fullerton, CA) Surface Area and Pore Size Analyzer using the BET method after degassing by heating at 180 °C for 3 h with He-gas purging.

### 2.4. Porosity, chemical stability determination, and membrane flux

Porosity of the prepared membrane was evaluated by Archimedes' principle. The prepared membrane is dried in air oven at 110 °C for 24 h to remove all moisture and its dry weight ($m_{dry}$) is determined. Then the membrane was immersed in deionized water for more than 24 h and taken out. Water on outer surface is removed using tissue paper and the wet weight of the membrane ($m_{wet}$) is measured. The porosity of the membrane was determined using the following equation: (Workneh and Shukla, 2008)

$$\varepsilon = \frac{m_{wet} - m_{dry}}{m_{dry}} \times 100\%$$

The chemical stability of prepared membranes was investigated by soaking membranes in HCl (1 M) and NaOH (1 M) solution at 60 °C for 4 week, individually. Samples were periodically removed from the solution every week and washed with distilled water to remove corrosion residues. Three measurements were performed for each sample. The weight of the membrane samples before and after soaking in HCl and NaOH solution was weighted after complete drying in a vacuum oven. The chemical stability was calculated from the average value according to the weight loss caused by the corrosion of acid and alkali (Bahaabad et al., 2014; George et al., 2005).

To determine the flux of obtained membrane, sintered membranes were set in a close contact fixation with rubber packing (a simple dead-end filtration setup). The effective filtration area was around 20 mm in diameter. Firstly, pure water was added on the top of membrane, and then a vacuum pump was used to drive the water cross the membrane. The weight of filtered water was weighted with time. Finally, the flux was calculated based on the weight changes.

## 3. Results and discussion

### 3.1. Phase transformation and composition of as-made alumina membrane

Fig. 1 showed the XRD patterns of the produced alumina membranes by treating boehmite (PDF# 74-1875) at temperatures of 450–1300 °C. γ-alumina (PDF# 74-2206) formed by the dehydration of boehmite and become the dominant phase when the membranes were treated at 450–650 °C. At 650–850 °C, weak peak intensity of bayerite ($Al(OH)_3$; PDF #83-2256) was detected. As bayerite can thermally transformed into boehmite even at low temperature of 200 °C (Du et al., 2009), the formation of bayerite during the sintering process was probably due to the instability of product phase(s) sintered at 650–850 °C, which might be vulnerable to the attack of moisture in the air during sample quenching (Lee et al., 1999; McHardy and Thomson, 1971). At 750 °C, the formation of small amount of δ-alumina (PDF# 46-1131) occurred in the sintered products. Although the peak intensity of δ-alumina increased at temperature increased from 750 to 950 °C, γ-alumina is still the dominant phase in the product. At 1100 °C, the peak of γ-alumina and δ-alumina almost disappeared, θ-alumina (PDF# 86-1410) became the dominant phase in the product with small amount of α-alumina. However, α-alumina (PDF# 74-1081) started to be the dominant phase in the products with small amount of θ-alumina when the temperature increased from 1100 to 1125 °C. At 1150 °C, θ-alumina almost disappeared, and a large amount of α-alumina formed. At 1300 °C, α-alumina become the dominant phase in the produced ceramic membrane (Boumaza et al., 2009).

As membrane properties may not only be effected by alumina structures but also by alumina contents in produced membranes,

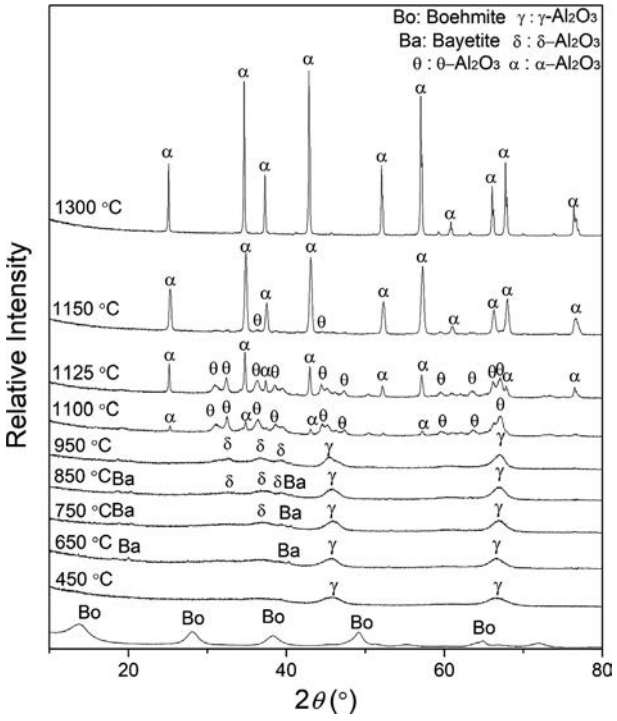


**Fig. 1.** XRD patterns for the produced alumina membranes by heating boehmite at 450–1300 °C for 0.5 h. Phase identification results indicated that the prepared alumina membrane experienced a series of transition from boehmite → γ-$Al_2O_3$ → δ-$Al_2O_3$ → θ-$Al_2O_3$ → α-$Al_2O_3$.

Rietveld refinement was used to determine the phase composition of the as-made membranes treated at temperature elevated from 450 to 1300 °C. The refinement fitting results of XRD patterns for the as-made membranes were presented in Fig. 2, and the satisfactory values of profile fitting are goodness of fit (GOF) values (Iyengar et al., 2001) in the range of 1.49–1.91 with $R_p < 6.68$. It is generally considered that the GOF value between 1.0 and 2.9 is satisfactory (Sahu and Panigrahi, 2011; Iwase et al., 2011). The graphical plots for Rietveld refinement presented in Fig. 2 suggest excellent agreement between the measured XRD data and the calculated XRD patterns by the Rietveld method. The results for quantitative analysis of alumina contents in the as-made membranes are plotted in Fig. 3. At 450 °C, the content of γ-alumina in the produced membrane was almost 100% indicated that most of boehmite transformed into γ-alumina in this sintering process. Although the content of γ-alumina decreased to around 90% when the temperature increased from 450 °C to 950 °C, γ-alumina was still the dominant phase in the as-made ceramic membrane. When the temperature increased from 650 to 950 °C, δ-alumina formed and the phase content increased from 5.1 to 10.8%. But the content of δ-alumina at each temperature was all quite low, which suggested that δ-alumina may formed as transition phase at the grain boundary of reactants due to the short sintering scheme (Kukukova et al., 2009). When the temperature increased from 950 to 1100 °C, the content of γ-alumina decreased dramatically from 89.2% to 56.3%, and the amount of θ-alumina increased quickly from 0 to 39.7%. Such result indicated that γ-alumina is gradually converted into θ-alumina via the formation of δ-alumina in the sintering process (Cai et al., 2003). At 1125 °C, the content of θ-alumina was around 61.6%, and α-alumina begun to substantially form. When temperature increased to 1150 °C, the content of θ-alumina decreased to around 8.3% and the amount of α-alumina increased dramatically to 87.6%. In the sintering process of 1125–1300 °C, θ-alumina continually transformed to be α-alumina. Finally, content

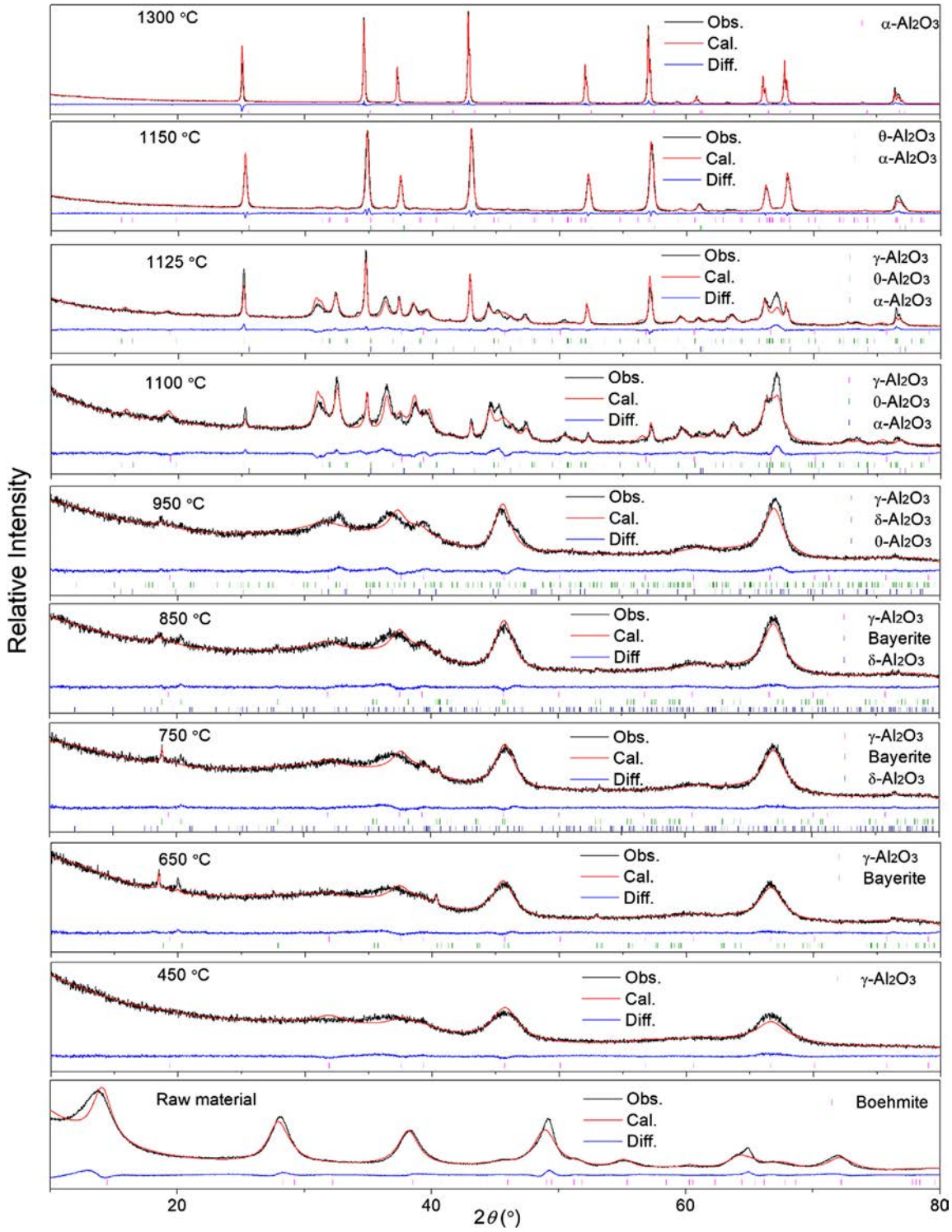


**Fig. 2.** Graphical plots of the Rietveld refinement for the produced alumina membranes by heating boehmite at 450–1300 °C for 0.5 h (blank line = experimental XRD pattern at different temperatures, red line = calculated XRD pattern, and blue line = difference curve between the experimental and calculated patterns). The vertical bars indicate the Bragg positions of the calculated reflections for different types of alumina. (For interpretation of the references to colour in this figure legend, the reader is referred to the web version of this article.)

of α-alumina increased to 99.8 wt% with the disappearance of other phases at 1300 °C. The results indicated the high purity of the 1300 °C sintered alumina membrane. The overall phase transformation of heating boehmite indicated that the prepared alumina membrane experienced a series of transition from boehmite → γ-alumina → δ-alumina → θ-alumina → α-alumina.

The crystalline size of different types of alumina in the as made-alumina membrane was calculated by the Rietveld refinement method, and illustrated at Fig. 4(a–d). As shown in Fig. 4(a), the average crystalline size of γ-alumina is around 3.8 nm at 450 °C, and stabilized at ~6 nm at 850–1125 °C. δ-alumina was with the stable average crystalline size of ~2.8 nm at 750–950 °C (Fig. 4

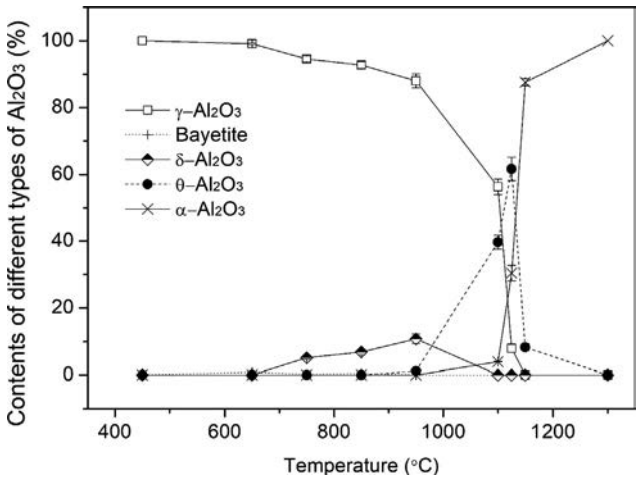


**Fig. 3.** Phase contents of different types of alumina in produced alumina membranes for heating boehmite at 450–1300 °C for 0.5 h.

(b)). In addition, the average crystalline size of θ-alumina quickly increased from 1.8 to 20.8 nm at 950–1125 °C (Fig. 4(c)). The α-alumina quickly increased from 56.5 nm to 106.3 nm from 1100 to 1300 °C (Fig. 4(d)). According to the variation of crystalline size and phase transformation, crystal growth and structure transformation of these different types of alumina was demonstrated in Fig. 5. Temperature was found to be critical for crystal growth in ceramic studies (Lee and Iqbal, 2001). The increased sintering temperature facilitated mass transfer mechanisms, like grain boundary diffusion and lattice diffusion (Shih and Leckie, 2007), thus, the conversions from boehmite to γ-alumina → δ-alumina → θ-alumina → α-alumina occurred at temperatures of 450–1300 °C. As shown in Fig. 5, three stage of the crystal growth in the sintering process was observed. Boehmite was firstly converted to γ- alumina at around 450 °C (Busca, 2014), and the significant formation of γ-alumina was observed at 450–850 °C. No significant change of phase transformation was detected at 650–850 °C, except the small growth of δ-alumina at 750 °C. This result was consistent with the formation temperature of δ-alumina reported by Pardo and Alarcón (2018). In the second stage, the decomposition of γ-alumina followed by the formation of θ-alumina was found at 950–1100 °C. The formation temperature (1100 °C) of θ-alumina was corresponded to the temperature determined by Pardo and Alarcón (2018). Finally, the transformation of θ-alumina into α-alumina was observed at 1125–1300 °C. When boehmite is used as precursor, the conversions from boehmite to α-alumina were complete at 1300 °C (Chagas et al., 2014). The significant phase transformation between different types of alumina may result in the change of the membrane properties (e.g. porosity, surface area, pore size and morphology) in the as-made alumina membrane.

### *3.2. Porosity, BET surface area, pore size and morphology of alumina membrane*

The porosity of as-made alumina membrane prepared at temperatures of 450–1300 °C was shown in Fig. 6 When the temperature increased from 450 to 850 °C, there is no significant change on the porosity of alumina ceramic membrane because of no significant change on the main phase in the as-made membrane (Fig. 3). When the temperature increased from 850 to 1300 °C, the porosity decreased quickly. Temperature increase led to the substantial phase transformation in the products, which is a strong

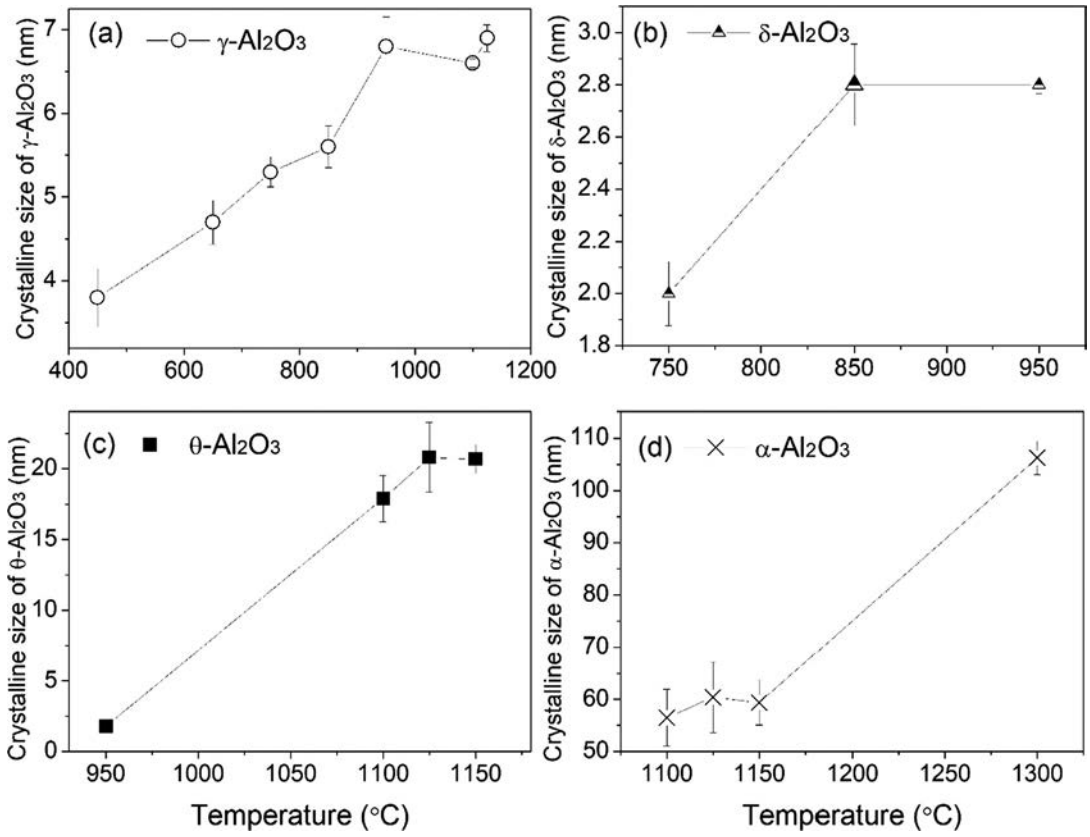


**Fig. 4.** Crystalline size of γ-$Al_2O_3$ (a), δ-$Al_2O_3$ (b), θ-$Al_2O_3$ (c) and α-$Al_2O_3$ (d) in produced alumina membranes for heating boehmite at temperature range of 450–1300 °C for 0.5 h.

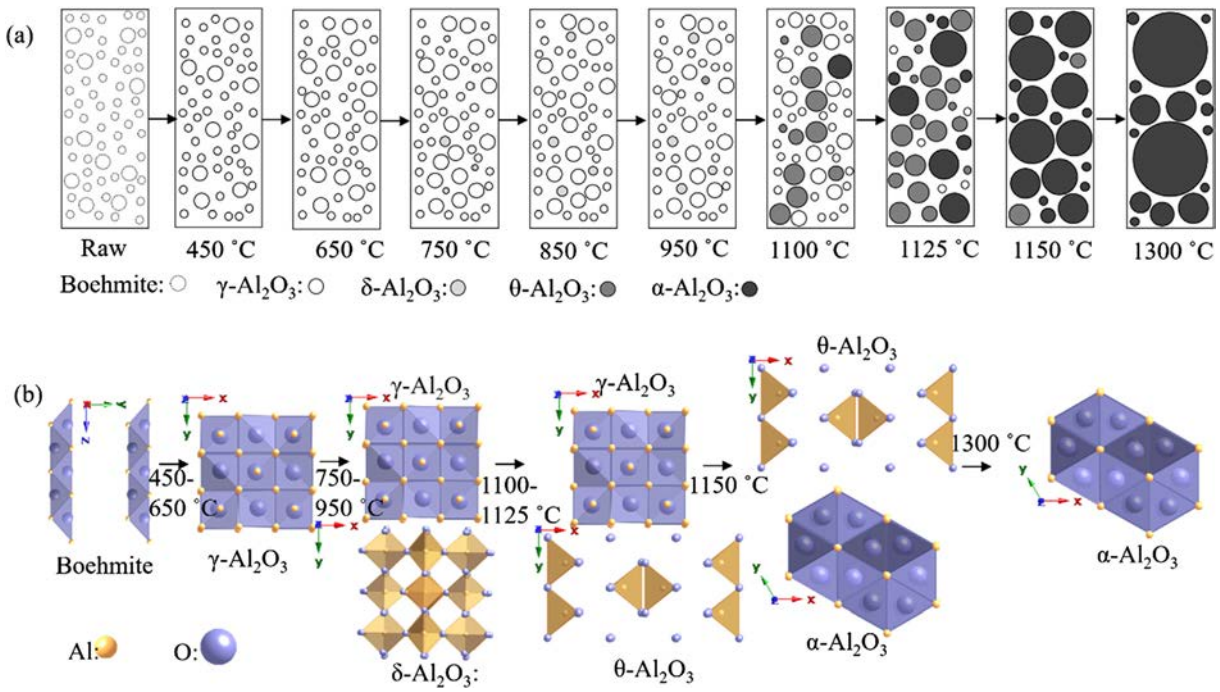


**Fig. 5.** Crystal growth (a) and phase transformation (b) of different types of alumina in produced alumina membranes for heating boehmite at 450–1300 °C for 0.5 h.

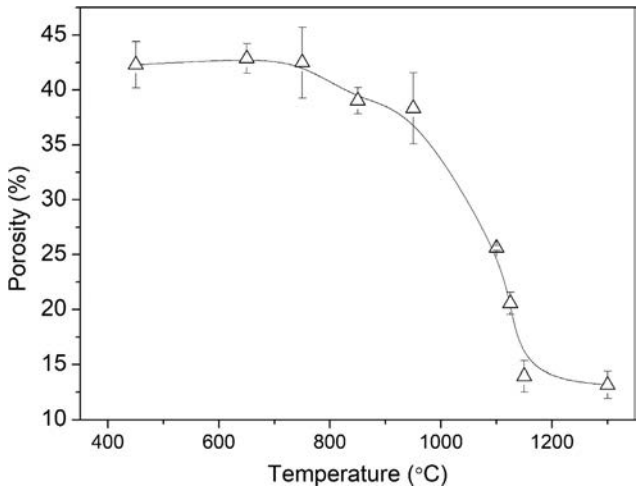


**Fig. 6.** Porosity of the prepared alumina membrane for heating boehmite at 450–1300 °C for 0.5 h.

mass transfer process. Such strong chemical reaction resulted in condense of ceramic membrane, which further led to the lower porosity in the as-made alumina membrane. Fig. 7 presented the scanning secondary electron micrographs of the surfaces of the as-made alumina membrane prepared at 450–1300 °C. At 450–650 °C, the transformation of beohmite to γ-alumina caused by the water evaporation of beohmite led to roughness nature of the produced membrane. However, the surface of alumina ceramic membrane has similarly porous textures (Fig. 7(a–c)) due to no phase change in the product at 450–750 °C. When temperature increased from 850 to 1300 °C, the surface of alumina ceramic membrane became more condensed due to the strong chemical reaction occurred in the as-made membrane (Fig. 7(d–i)). The cross-section images of alumina membranes obtained at temperatures of 450–1300 °C were provided in Fig. 8. The cross-section images were similar with the surface images due to the uniform distribution of beohmite. Similarly, almost no texture change was found in 450–750 °C products (Fig. 8(a–c)). Whereas, with temperature elevated from 850 to 1300 °C (Fig. 8(d–i)), the observed pore size of alumina membrane was reduced, and alumina membrane became more compact due to the robust sintering process.

Fig. 9 showed the BET surface area and pore size of alumina ceramic membrane obtained at temperatures of 450–1300 °C. When the temperature increased to 450 °C, the surface area of the produced membrane increased quickly. The treated temperature (450 °C) led to a quick evaporation of water decomposed from boehmite to γ-alumina. However, when the temperature increased from 450 to 850 °C, the surface area had no significant change. Fig. 1 indicated that γ-alumina is the main phase at 450–850 °C, and no significant change of the surface area in the produced membrane maybe caused by no phase transformation occurred at this sintering process. When the temperature increased from 850 to 1300 °C, the surface area of as-made alumina membrane decreased dramatically. It should be attributed to the strong chemical reaction occurred in the heating process, which condensed the alumina membrane. It had been proven that higher temperature treatment can lead to the decrease of surface area in alumina nanoparticles (Zhang et al., 2008). Fig. 9 also showed that the total pore size of the as-made membrane decreased with the increase of temperature, which was also strong evidence of the potential condense effect initialed by the higher temperature treatment. One interesting finding is that the surface area decreased and the total pore size increased with the temperature elevated from 450 to 650 °C. The increase of total pore size indicated that the water evaporation increased the pore size of as-made membrane. At higher temperatures (750–1300 °C), the condense effect initialed by the temperature increase lead to the decrease of total pore size in the as-made membrane.

### 3.3. Chemical stability and membrane flux

Due to the corrosion of acid and alkali, the weight loss of as-made alumina ceramic membrane obtained at temperature from

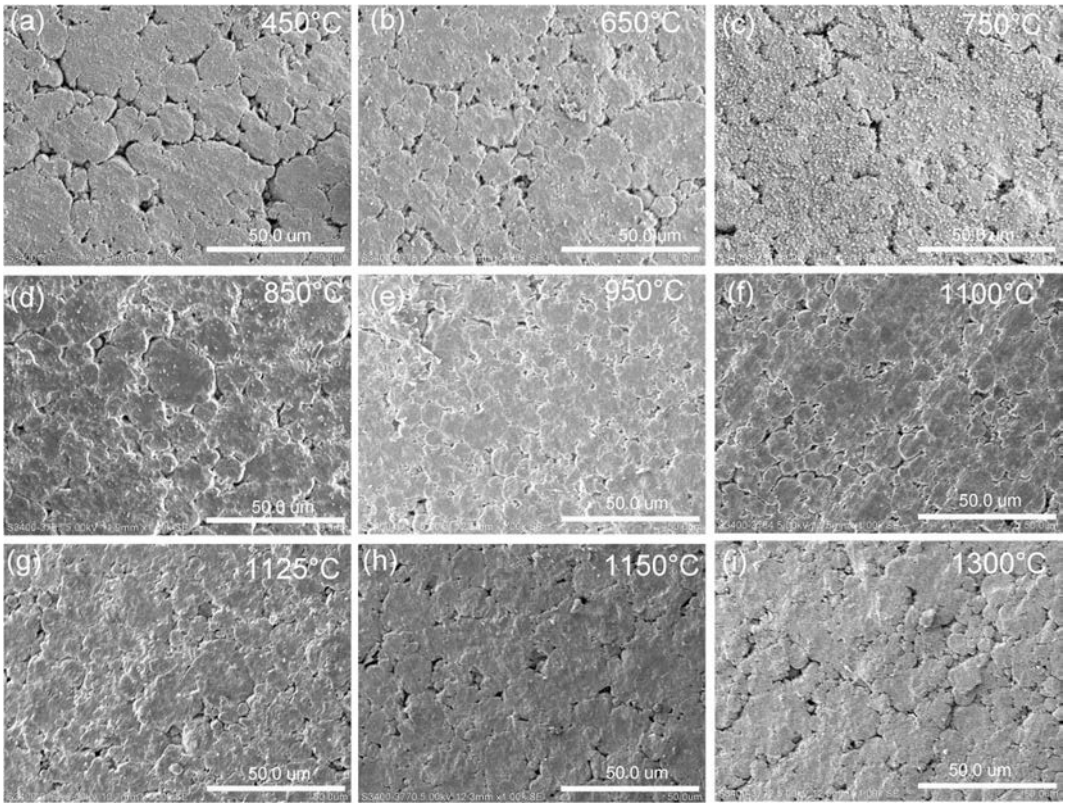


**Fig. 7.** The morphology of alumina-based ceramic membrane obtained at temperature ranged from 450 to 1300 °C.

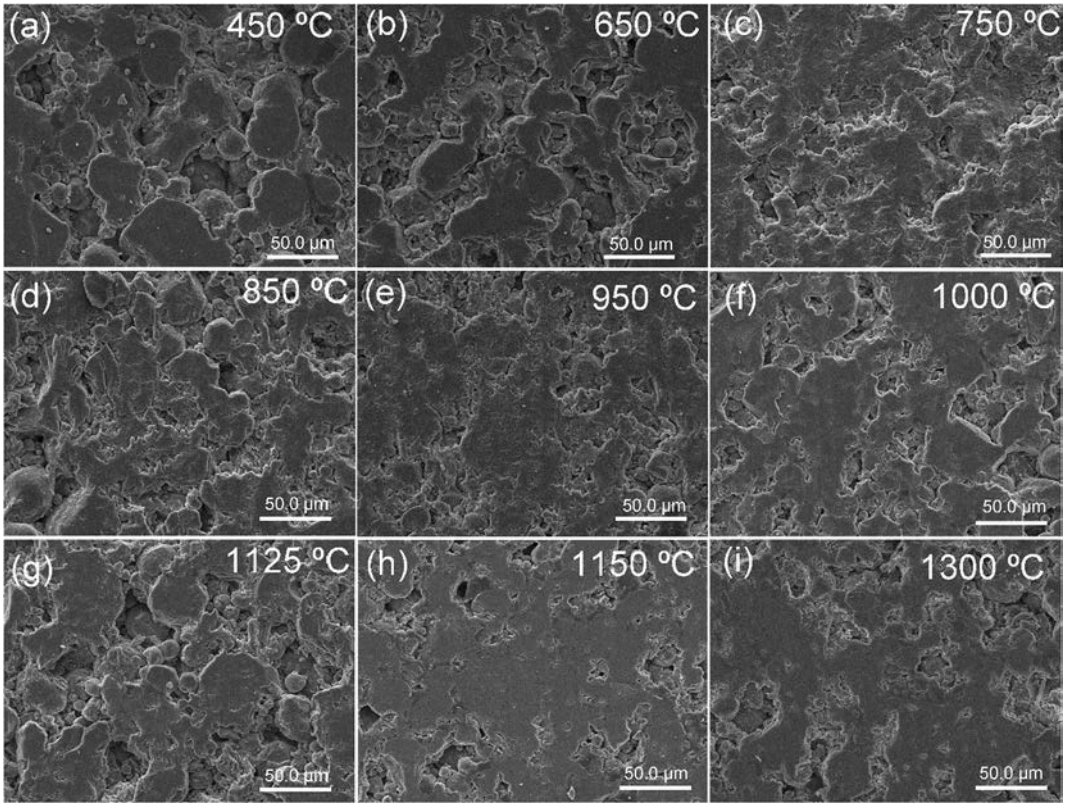


**Fig. 8.** The cross-section images of alumina-based ceramic membrane obtained at temperature ranged from 450 to 1300 °C.

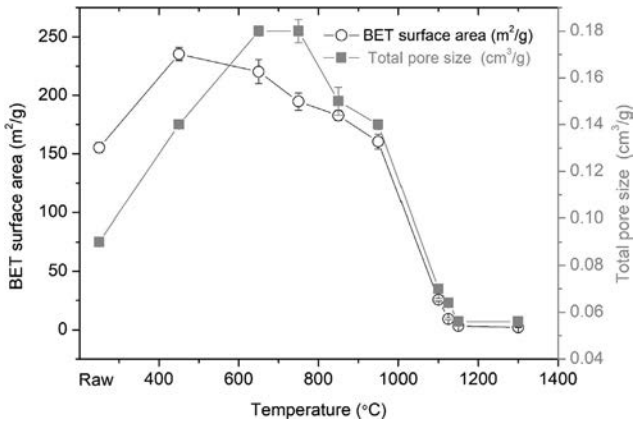


**Fig. 9.** BET and pore size of the prepared alumina membranes for raw boehmite and heated boehmite at 450–1300 °C for 0.5 h.

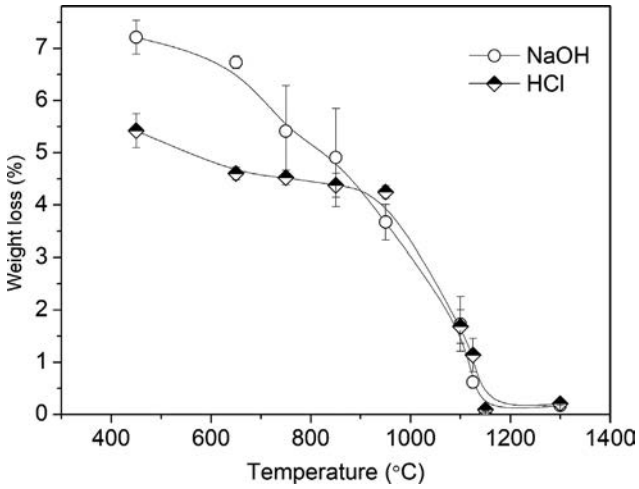


**Fig. 10.** Chemical stability of the prepared alumina membranes for raw boehmite and heated boehmite at 450–1300 °C for 0.5 h.

450 to 1300 °C was shown in Fig. 10. Alumina ceramic membranes obtained at lower temperatures (450–850 °C) lost their weight quickly, which should be attributed to the lower tolerate of γ-alumina in acid and alkaline solutions.

As the temperature increased, the transformation of γ-alumina into θ-alumina and α-alumina led to the higher stability of ceramic membrane even in acid and alkaline conditions. Combined with the results of XRD patterns in Fig. 1 and chemical stability in Fig. 10, it can be interpreted that higher temperature alumina products usually had higher stability than lower temperature ones. It should be noted that α-alumina had the highest chemical stability than other types of alumina. Another phenomenon is that the lower temperature products are more stable in acid condition than alkaline ones, which indicated that the as-made products are more appropriately used in acid conditions.

The pure water flux of each alumina ceramic membrane obtained at temperatures of 450–1300 °C was shown Fig. 11. The original membrane made by boehmite showed a very high flux of 8536 $L{\cdot}m^{-3}{\cdot}h{\cdot}bar$. As a dry pressing method was used for the original membrane, the interspace between boehmite particles in the un-sintered products led to the high pure water flux. When the membrane was sintered at 450 °C, the pure water flux decreased dramatically to be around 4673 $L{\cdot}m^{-3}{\cdot}h{\cdot}bar$. The decrease of water flux was caused by the condense effect initialed by the heating process. The mass transfer during the transformation from boehmite to γ-alumina led to the reduction of interspace

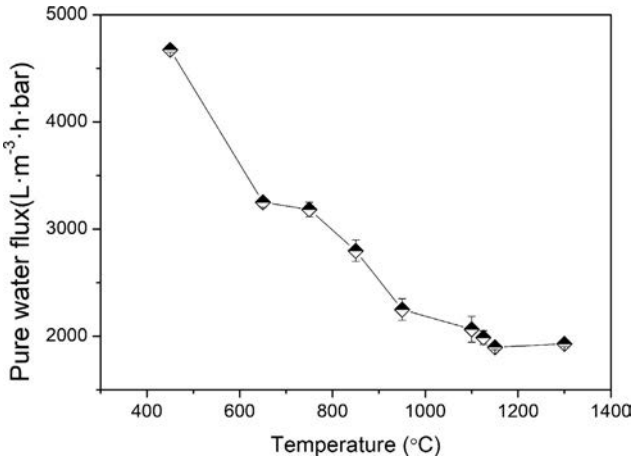


**Fig. 11.** The pure water flux of the produced alumina membranes obtained at 450–1300 °C for 0.5 h.

of the alumina membrane. Although the water evaporation of boehmite in the transformation process would produce some pores in the ceramic membrane, the reduction of pure water flux in the as-made alumina ceramic membrane was detected with the temperature increased from 450 to 850 °C. Thus, the potential condense effect would be the main mechanism for the reduction of pure water flux of the as-made alumina ceramic membrane as the increase of temperature. The pure water flux of products obtained at different temperatures of 450–1300 °C is in the range of 1896–4673 $L{\cdot}m^{-3}{\cdot}h{\cdot}bar$, which is similar to the pure water flux of alumina-based ceramic membrane (from 1000 to 4000 $L{\cdot}m^{-3}{\cdot}h{\cdot}bar$) made by Ha et al. (2018). However, their ceramic membrane is made by α-alumina, which may consume large amounts of heat (>1300 °C) during sintering processes. As shown in Fig. 11, the lowest permeate flux is obtained for ceramic membrane prepared at firing temperature 1150 °C. The permeate flux of other prepared ceramic membranes obtained at 1100, 1125 and 1300 °C are fairly close to each other being respectively (2064, 1986, and 1928) $L{\cdot}m^{-3}{\cdot}h{\cdot}bar$ because of the similar phase compositions in these temperatures. The organic rejection ability of as-made ceramic membrane treated at different temperature was evaluated by using a filtration test fed with 1000 mg/L BSA solution. The BSA rejection efficiencies of ceramic membranes treated from 450 to 1300 °C ranged from 18.1% to 37.0%, which is similar to those of common ultrafiltration membrane. Compared to ceramic membrane made by α-alumina, this study provided lower temperature products made by boehmite, which also showed similar chemical and physical properties. This study demonstrated a preferred strategy to reduce the cost of alumina-based ceramic membrane.

## 4. Conclusions

Alumina ceramic membrane was prepared by firing the disc form of boehmite at temperatures of 450 to 1300 °C for 0.5 h. The produced membrane was analyzed by QXRD for phase composition and crystalline size distribution, which proved that the alumina ceramic membranes experienced a series of crystal growth from γ-alumina → δ-alumina → θ-alumina → α-alumina at 450–1300 °C. Then the prepared ceramic membranes were characterized for their physical parameters and microstructure. The results indicated that membrane properties shown no obvious change at 450–850 °C products, because of no significant phase transformation in membrane products. However, the significant change in membrane properties is corresponding to the change of phase con-

tent at 900–1300 °C heated membrane products. The results indicated that properties of alumina membrane were greatly influenced by the formed alumina phases and theirs crystallize size. Generally, lower temperature (1150 °C) membrane had similar properties as the 1300 °C treated product, which are proposed to offer good application future for water purification.

## Declaration of interest

The author declares that there is no conflict of interest.

## Acknowledgements

This research was supported by Science and Technology Program of Guangzhou, China (201804010103), Special Fund for Soil Pollution and Control of Shaoguan, China (2017sgtyfz302), the Research Fund Program of Guangdong Provincial Key Laboratory of Environmental Pollution Control and Remediation Technology (2018K18), and the Fundamental Research Funds for the Central Universities.

## References

Abdullah, N., Rahman, M.A., Othman, M.H.D., Jaafar, J., Aziz, A.A., 2018. Preparation, characterizations and performance evaluations of alumina hollow fiber membrane incorporated with UiO-66 particles for humic acid removal. J. Memb. Sci. in press.

Achiou, B., Elomari, H., Bouazizi, A., Karim, A., Ouammou, M., Albizane, A., Bennazha, J., Alami Younssi, S., El Amrani, I.E., 2017. Manufacturing of tubular ceramic microfiltration membrane based on natural pozzolan for pretreatment of seawater desalination. Desalination 419, 181–187.

Achiou, B., Beqqour, D., Elomari, H., Bouazizi, A., Ouammou, M., Bouhria, M., Aaddane, A., Khiat, K., Younssi, S.A., 2018. Preparation of inexpensive NaA zeolite membrane on pozzolan support at low temperature for dehydration of alcohol solutions. J. Environ. Chem. Eng. 6 (4), 4429–4437.

Antsiferoz, V.N., Gilev, V.G., 2001. Membrane porous materials from sialon. Refract. Ind. Ceram. 42, 57–63.

Bahaabad, M.S., Nasaj, E.T., Falamaki, K., Zakeri, A., 2014. Corrosion properties of $70SiO_2$-$15TiO_2$-$15ZrO_2$ ceramic membrane. J. Adv. Mater. Process 2, 15–26.

Barma, S., Mandal, B., 2014. Effects of sintering temperature and initial compaction load on alpha-alumina membrane support quality. Ceram. Int. 40, 11299–11309.

Boudaira, B., Harabia, A., Bouzerara, F., Zenikheri, F., Foughali, L., Guechi, A., 2016. Preparation and characterization of membrane supports for microfiltration and ultrafiltration using kaolin (DD2) and $CaCO_3$. Desalin. Water Treat 57, 5258–5265.

Boumaza, A., Favaro, L., Lédion, J., Sattonnay, G., Brubach, J.B., 2009. Transition alumina phases induced by heat treatment of boehmite: an X-ray diffraction and infrared spectroscopy study. J. Solid State Chem. 182, 1171–1176.

Busca, G., 2014. Structural, surface, and catalytic properties of aluminas. Adv. Catal. 57, 319–404.

Cai, S., Rashkeev, S.N., Pantelides, S.T., Sohlberg, K., 2003. Phase transformation mechanism between γ- and θ-alumina. Phys. Rev. B 67, 224104.

Chagas, L.H., De Carvalho, G.S.G., Gil, R.A.S.S., Chiaro, S.S.X., Leitao, A.A., Diniz, R., 2014. Obtaining aluminas from the thermal decomposition of their different precursors: an Al-27 MAS NMR and X-ray powder diffraction studies. Mater. Res. Bull. 49, 216–222.

Chang, Y.F., Wu, J., Zhang, M., Kupp, E., Messing, G.L., 2017. Molten salt synthesis of morphology controlled alpha-alumina platelets. Ceram. Int. 43, 12684–12688.

Chen, R., Li, Y., Zhao, Y., Li, S.J., Xiang, R.F., Xu, N.N., Liu, F., 2017. Effect of inorganic acid on the phase transformation of alumina. J. Alloy Compd. 699, 170–175.

Cowan, M.G., Gin, D.L., Noble, R.D., 2016. Poly (ionic liquid)/ionic liquid ion-gels with high "free" ionic liquid content: platform membrane materials for $CO_2$/light gas separations. Accounts Chem. Res. 49, 724–732.

De La Torre, A.G., Bruque, S., Aranda, M.A.G., 2001. Rietveld quantitative amorphous content analysis. J. Appl. Crystallogr. 34 (2), 196–202.

Del Colle, R., Fortulan, C.A., Fontes, S.R., 2011. Manufacture and characterization of ultra and microfiltration ceramic membranes by isostatic pressing. Ceram. Int. 37, 1161–1168.

Dong, Z., Meng, J., Zhu, H., Yuan, G., Cong, Y., Zhang, J., Li, X., Westwood, A., 2017. Synthesis of SiC nanowires via catalyst-free pyrolysis of silicon-containing carbon materials derived from a hybrid precursor. Ceram. Int. 43, 11006–11014.

Du, X., Su, X., Wang, Y., Li, J., 2009. Thermal decomposition of grinding activated bayerite. Mater. Res. Bull. 44, 660–665.

Fu, L., Gu, H., Huang, A., Zhang, M., Li, Z., 2015. Slag resistance mechanism of lightweight microporous corundum aggregate. J. Am. Ceram. Soc. 98, 1658–1663.

George, J., Ramana, K.V., Sabapathy, S.N., Jagannath, J.H., Bawa, A.S., 2005. Characterization of chemically treated bacterial (Acetobacter xylinum) biopolymer: some thermo-mechanical properties. Int. J. Biol. Macromol. 37, 189–194.

Gestel, T.V., Vandecasteele, C., Buekenhoudt, A., 2003. Corrosion properties of alumina and titania NF membranes. J. Membr. Sci. 214, 21–29.

Ha, J.H., Bukhari, S.Z.A., Lee, J., Song, I.H., 2018. The membrane properties of alumina-coated alumina support layers and alumina-coated diatomite-kaolin composite support layers. Adv. App. Ceram. 117, 1–8.

Hao, Z., Wu, B., Wu, T., 2018. Preparation of alumina ceramic by κ-$Al_2O_3$. Ceram. Int. 44, 7963–7966.

Hashimoto, H., Kojima, S., Sasaki, T., Asoh, H., 2018. α-Alumina membrane having a hierarchical structure of straight macropores and mesopores inside the pore wall. J. Eur. Ceram. Soc. 38, 1836–1840.

Hemmer, E., Kumakiri, I., Lecerf, N., Bredesen, R., Barth, S., Altmayer, J., Donia, N., Cavelius, C., Soga, K., Mathur, S., 2012. Nanostructured $ZrO_2$ membranes prepared by liquid-injection chemical vapor deposition. Micropor. Mesopor. Mat. 163, 229–236.

Hossain, F.M., Riley, D.P., Murch, G.E., 2005. Ab initio calculations of the electronic structure and bonding characteristics of $LaB_6$. Phys Rev B 72, 235101.

Huang, S.C., Huang, C.T., Lu, S.Y., Chou, K.S., 1999. Ceramic/polyaniline composite porous membranes. J. Porous Mater. 6, 153–159.

Hubadillah, S.K., Othman, M.H.D., Matsuura, T., Rahman, M.A., Harun, Z., 2018. Fabrications and applications of low cost ceramic membrane from kaolin: a comprehensive review. Ceram. Int. 44, 4538–4560.

Isobe, T., Kameshima, Y., Nakajima, A., Okada, K., Hotta, Y., 2006. Extrusion method using nylon 66 fibers for the preparation of porous alumina ceramics with oriented pores. J. Eur. Ceram. Soc. 26 (12), 2213–2217.

Issaoui, M., Limousy, L., 2018. Low-cost ceramic membranes: synthesis, classifications, and applications. Comptes Rendus Chimie. In press.

Iwase, K., Sakaki, K., Matsuda, J., Nakamura, Y., Ishigaki, T., 2011. Synthesis and crystal structure of a Pr5Ni19 superlattice alloy and its hydrogen absorption–desorption property. Inorg. Chem. 50, 4548–4552.

Iyengar, S.S., Phadnis, N.V., Suryanarayanan, R., 2001. Quantitative analyses of complex pharmaceutical mixtures by the Rietveld method. Powder. Diffr. 16, 20–24.

Jedidi, I., Khemakhem, S., Larbot, A., Amar, R.B., 2009a. Elaboration and characterisation of fly ash based mineral supports for microfiltration and ultrafiltration membranes. Ceram. Int. 35 (7), 2747–2753.

Jedidi, I., Saïdi, S., Khemakhem, S., Larbot, A., Elloumi-Ammar, N., Fourati, A., Charfi, A., Ben Salah, A., Ben, Amara R., 2009b. Elaboration of new ceramic microfiltration membranes from mineral coal fly ash applied to waste water treatment. J. Hazard. Mater. 172, 152–158.

Kim, J., Van der Bruggen, B., 2010. The use of nanoparticles in polymeric and ceramic membrane structures: review of manufacturing procedures and performance improvement for water treatment. Environ. Pollut. 158, 2335–2349.

Kujawa, J., Cerneaux, S., Koter, S., Kujawski, W., 2014. Highly efficient hydrophobic titania ceramic membranes for water desalination. Appl. Mater. Inter. 6, 14223–14230.

Kukukova, A., Aubin, J., Kresta, S.M., 2009. A new definition of mixing and segregation: three dimensions of a key process variable. Chem. Eng. Res. Des. 87, 633–647.

Lee, A., Elam, J.W., Darling, S.B., 2016. Membrane materials for water purification: design, development, and application. Environ. Sci. Wat. Res. Tech. 2, 17–42.

Lee, S.K., Lee, S.B., Park, S.Y., Yi, Y.S., Ahn, C.W., 2009. Structure of amorphous aluminum oxide. Phys. Rev. Lett. 103, 095501.

Lee, W., Park, S.J., 2014. Porous anodic aluminum oxide: anodization and templated synthesis of functional nanostructures. Chem. Rev. 114, 7487–7556.

Lee, W.E., Iqbal, Y., 2001. Influence of mixing on mullite for;mation in porcelain. J. Eur. Ceram. Soc. 21, 2583–2586.

Lee, Y.P., Liu, Y.H., Yeh, C.S., 1999. Formation of bayerite, gibbsite and boehmite particles by laser ablation. Phys. Chem. Chem. Phys. 1, 4681–4686.

Levin, I., Brandon, D., 1998. Metastable alumina polymorphs: crystal structures and transition sequences. J. Am. Ceram. Soc. 81, 1998–2012.

Lima, M.M.R.A., Monteiro, R.C.C., Graça PF, M., da Silva, M.F., 2012. Structural, electrical and thermal properties of borosilicate glass-alumina composites. J. Alloy Compd. 538, 66–72.

Magallanes-Perdomo, M., Carrodeguas, R.G., Pena, P., De Aza, P.N., De Aza, S., De Aza, A.H., 2009. Non-isothermal devitrification study of wollastonite-tricalcium phosphate bioeutectic® glass. Key Eng. Mater. 396–398, 127–130.

McHardy, W.J., Thomson, A.P., 1971. Conditions for the formation of bayerite and gibbsite. Mineral Mag. 38, 358–368.

Mouiya, M., Abourriche, A., Bouazizi, A., Benhammou, A., El Hafiane, Y., Abouliatim, Y., Nibou, L., Oumam, M., Ouammou, M., Smith, A., Hannache, H., 2018. Flat ceramic microfiltration membrane based on natural clay and Moroccan phosphate for desalination and industrial wastewater treatment. Desalination 427, 42–50.

Nel, R.J., de Klerk, A., 2009. Dehydration of C5–C12 linear 1-alcohols over η-alumina to fuel ethers. Ind. Eng. Chem. Res. 48, 5230–5238.

Nishihora, R.K., Rachadel, P.L., Quadri, M.G.N., Hotza, D., 2018. Manufacturing porous ceramic materials by tape casting-a review. J. Eur. Ceram. Soc. 38 (4), 988–1001.

Padaki, M., Murali, R.S., Abdullah, M.S., Misdan, N., Moslehyani, A., 2015. Membrane technology enhancement in oil–water separation. A review. Desalination 357, 197–207.

Pardo, P., Alarcón, J., 2018. Thermal stability of transition alumina nanocrystals with different microstructures. Ceram. Int. 44 (10), 11486–11496.

Raman, L.P., Cheryan, M., Rajagopalan, N., 2011. Consider nanofiltration for membrane separations. Chem. Eng. Progr. 211, 83–90.
Rendtorff, N.M., Conconi, M.S., Aglietti, E.F., Chain, C.Y., Pasquevich, A.F., Rivas, P.C., Martínez, J.A., Caracoche, M.C., 2010. Phase quantification of mullite-zirconia and zircon commercial powders using PAC and XRD techniques. Hyperfine Interact 198 (1), 211–218.
Sahu, N., Panigrahi, S., 2011. Mathematical aspects of Rietveld refinement and crystal structure studies on $PbTiO_3$ ceramics. Bull. Mater. Sci. 34, 1495–1500.
Shih, K., Leckie, J.O., 2007. Nickel aluminate spinel formation during sintering of simulated Ni-laden sludge and kaolinite. J. Eur. Ceram. Soc. 27 (1), 91–99.
Tantau, L.J., Islam, M.T., Payne, A.T., Tran, C.Q., Cheah, M.H., 2014. High accuracy energy determination and calibration of synchrotron radiation by powder diffraction. Radiat. Phys. Chem. 95, 73–77.
Téllez-Vázquez, J.O., Patiño-Carachure, C., Rosas, G., 2016. Alumina nanowire growth by water decomposition and the peritectic reaction of decagonal $Al_{65}Cu_{15}Co_{20}$ quasicrystals. Mater. Charact. 112, 155–159.
Vega, V., Gelde, L., González, A.S., Prida, V.M., Hernando, B., Benavente, J., 2017. Diffusive transport through surface functionalized nanoporous alumina membranes by atomic layer deposition of metal oxides. J. Ind. Eng. Chem. 52, 66–72.
Wang, Y., Wang, J., Shen, M., Wang, W., 2009. Synthesis and properties of thermostable γ-alumina prepared by hydrolysis of phosphide aluminum. J. Alloy Compd. 467, 405–412.
Weber, R., Chmiel, H., Mavrov, V., 2013. Characteristics and application of new ceramic nanofiltration membranes. Desalination 157, 113–125.
Wei, Z., Hou, J., Zhu, Z., 2016. High-aluminum fly ash recycling for fabrication of cost-effective ceramic membrane supports. J. Alloy Compd. 683, 474–480.
Workneh, S., Shukla, A., 2008. Synthesis of sodalite octahydrate zeolite-clay composite membrane and its use in separation of SDS. J. Membr. Sci. 309, 189–195.
Xia, C., Liu, M., 2001. A simple and cost-effective approach to fabrication of dense ceramic membranes on porous substrates. J. Am. Ceram. Soc. 84, 1903–1905.
Yang, H., Liu, M., Ouyang, J., 2010. Novel synthesis and characterization of nanosized γ-$Al_2O_3$ from kaolin. Appl. Clay Sci. 47, 438–444.
Zawrah, M.F., Khattab, R.M., Girgis, L.G., Shereefy, E.E.E., Sawan, S.E.A., 2017. Synthesis of anatase nano wire and its application as a functional top layer for alumina membrane. Ceram. Int. 43, 17104–17110.
Zhang, X., Honkanen, M., Levänen, E., Mäntyla, T., 2008. Transition alumina nanoparticles and nanorods from boehmite nanoflakes. J. Cryst. Growth 310, 3674–3679.